Photocatalytic Hydrogen Production Based on a Serial Metal-Salen Complexes and the Reaction Mechanism

Cheng-Bo Li,*[a] Yilong Chu, [a] Jinjiao He,[a] Jijia Xie, [b] Jiawei Liu,[a] Ning Wang,[a] and Junwang Tang*[b]

Abstract: Three metal-salen (Ni, Cu, Zn) complexes were firstly introduced into homogeneous photocatalytic hydrogen-evolution systems. Based on these complexes, we developed noble-metal-free hydrogen production systems using disodium salts of Eosin Y (EY^{2-}) as photosensitizers and trimethylamine (TEA) as sacrificial donors. In a Ni(II)-salen/EY^{2-}/TEA system, a TON of 362 basd on Ni(II)-salen was achieved in 5.5 h with one time complement for EY^{2-}. The stability study revealed the quick photodecomposition of EY^{2-} in the presence of ether Ni(II)-salen, TEA or both chemicals, and quick dehalogenation of EY^{2-} was observed in the presence of TEA under irradiation. Besides, relatively slower photodecomposition of Ni(II)-salen was also found. These factors should be responsible for the deactivation of the photolysis system. Investigation of electrocatalytic proton reduction by Ni(II)-salen showed a CECE mechanism. An overall catalytic rate constant of 7.62×10^6 M^{-2} s^{-1} was achieved. Combined with the stability analysis, photo-induced electron transfer and electrochemistry investigation, for the first time, the photocatalytic hydrogen production mechanism for metal-salen complexes (e.g. Ni(II)-salen) was proposed.

Introduction

There has been intense effort to develop artificial photosynthesis that can make use of solar energy to provide clean and renewable alternatives to fossil fuels.[1] Hydrogen is an important candidate as a fuel for prospective electrochemical devices, such as proton exchange membrane fuel cells.[2] H_2 can also be produced via photochemical water splitting, offering a promising approach to sustainable energy storage by solar cells.[3] Both electrochemical and solar systems rely on the development of effective hydrogen evolution catalysts, including molecular complexes. Platinum, in a positive way, is an excellent and versatile catalyst for H_2 production, but the scarcity and high cost of noble metals pose serious limitations to its widespread use.[4] Considering the demand for large-scale hydrogen production in the future, developing catalysts based on earth-abundant metals to replace Pt allured great interesting.[5] Nature demonstrates how to use earth-abundant metallic elements in combination with proteins to capture sunlight, and then to store its energy in H_2.[6] Inspired by natural photosynthesis, a colorful array of iron, nickel and cobalt complexes have been crafted for hydrogen evolving catalysts, many of which show outstanding turnover frequencies and catalytic lifetimes.[7] However, for molecular systems, the majority still employ noble or rear metals used in photosensitizer (PS) such as Pt,[8] Ru,[9] Ir,[10] Os,[11] Re[12] etc. Especially, in order to thoroughly excavate catalysts' catalytic ability, PS containing noble metals are usually used several times' scale over catalysts in a multi-components system, which greatly increases the cost of hydrogen production systems. To this end, noble-metal-free hydrogen production systems have been developed using organic dyes (e.g. Eosin Y (EY^{2-}),[13] Rose Bengal (RB^{2-}),[13a-d] Erythrosin B (EB^{2-}),[13a, 13c, 13i] Fluorescein (Fl^{2-}),[13c, 14] Rhodamine[15], Erythrosin yellowish (ErY),[16] and other synthesized organic dyes[17]) or metal-organic dyes.[18] Yet many homogeneous catalytic systems are still being designed with synthetically challenging and costly ligand manifolds which are unsuitable for implementation at scale.[17e] An ideal system would require minimal synthetic effort, only inexpensive compounds or materials, and have the capability to be directly tied to a renewable energy source to produce clean H_2 without further modification.[19]

Salen ligands, with four coordinating sites and two axial sites open to ancillary ligands, could control the performance of metals in a large variety of useful catalytic transformations and are able to stabilize many metals in various oxidation states.[20] Moreover, they can be prepared simply in one step from the reaction of an aldehyde with a diamine (followed by filtration).[21] Many mononuclear and multinuclear metal-salen complexes have been used in organic catalytic reactions,[21-22] while their utilization in water spitting has rarely been developed.[17e, 23] Recently, we reported a noble-metal-free hydrogen production systems based on cobalt-salen complex, in which xanthene dyes are usually introduced as photosensitizers.[17e] The system presented good activity compared to other well-known cobalt complexes in noble-metal-free systems. However, the detailed electrochemical behavior of the complex and the possible mechanism of H_2 production catalysis have not been probed yet. More hydrogen production systems based on metal-salen complexes remain to be developed and investigated in detail by photochemistry and electrochemistry. Here, we report another three metal-salen complexes (Ni(II)-, Cu(II)- and Zn(II)-salen) which are introduced into photocatalytic hydrogen evolution systems containing EY^{2-} as PS and TEA or TEOA as sacrificial donors. Their photocatalytic hydrogen evolving performace and stability are thoroughly investigated. Furthermore, electrocatalytic hydrogen evolving performaces based on Ni(II)−salen complex are investigated. Finally, based on the UV-vis, electrochemical and fluoresence-quenching analysis, we proposed a mechanism for the photocatalytic H_2 evolution.

[a] Dr. Cheng-Bo Li, Yilong Chu, Jinjiao He, Dr. Jiawei Liu and Dr. Ning Wang
Key Lab of Synthetic and Natural Functional Molecule Chemistry of Ministry of Education, The Energy and Catalysis Hub
College of Chemistry and Materials Science, Northwest University, Xi'an 710069, P. R. China.
E-mail: lcb123@mail.edu.cn

[b] Prof. Junwang Tang and Dr. Jijia Xie
Department of Chemical Engineering
UCL
Torrington Place, London WC1E 7JE, UK
E-mail: Junwang.tang@UCL.AC.UK

Supporting information for this article is given via a link at the end of the document.

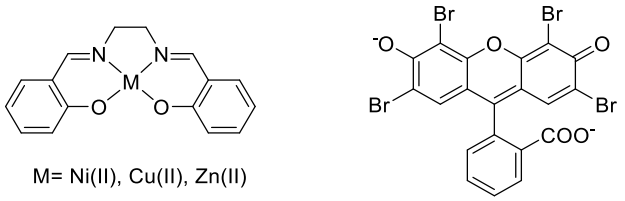

Scheme 1. Structures of metal–salen complexes and EY^{2-} used in present work.

Results and Discussion

Photocatalytic hydrogen generation

Photocatalytic hydrogen generation experiments were carried out under 450 nm LED at 298 K in water/MeOH (2/1, v/v) with relative concentrations of EY/Cat=10/1, in the presence of TEA or TEOA as the electron donors. The produced H_2 was quantified by gas chromatography (GC) analysis of the headspace gas mixture; this was then used to calculate the turnover number (TON) versus the catalyst. Our previous work has shown that the system EY^{2-}/Co(II)-salen/TEA is pH-dependent and the highest catalytic activity presented at pH 10.[17e] Hence, in the present work, we conducted the hydrogen-evolving reactions at pH 10. Control experiments (based on Ni(II)-salen complex) in the absence of either EY^{2-} or TEA (or TEOA) presented no detectable hydrogen (Figure S1).

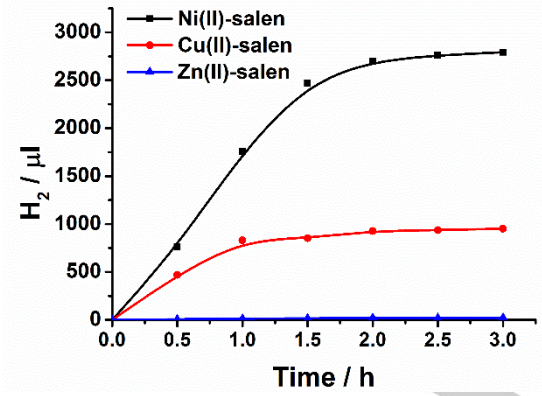

Figure 1. Photocatalytic H_2 production comparison of Ni(II)-alen, Cu(II)-salen and Zn(II)-salen complexes (0.1 mM) with EY^{2-} (1 mM) and 10% TEA, at pH 10.

Initial photochemical hydrogen-evolution experiment was carried out in the presence of EY^{2-} (1 mM), Ni(II)-salen (0.1 mM), TEA (10%, v/v) and 5 mL MeOH/H_2O (1: 2, v/v) at pH 10. A relative high TON of 250 was achieved in 3 h irradiation, corresponding to 2.8 mL of H_2 generated (Figure 1). To compare the efficiency of Ni(II)-salen to Cu(II)-salen and Zn(II)-salen, these catalysts were tested under the identical experimental conditions with an EY^{2-}/cat. ratio of 10 : 1. The pH values were kept at 10 which likewise were the optimal pH value for these reactions, as shown previously.[17e] Under these conditions, the Cu(II)-salen, with a TON of 85, turns out to be much less active than Ni(II)-salen (Figure 1). While the Zn(II)-salen, with a TON of 2, is over 100 times less active than the Ni(II)-salen system. The fact that the Ni(II)-salen system displays the highest catalytic performance in comparison to the other two catalytic systems should be due to the metal nature of the complexes. Nevertheless, compared to other Ni complexes in photocatalytic systems using EY^{2-} as PS and TEA as sacrificial agents, our complex shows a very compatitive activity. For example, Fan and co-authors reported a Ni dithiolene complex, namely $N^tBu_4[Ni(BNT)_2]$ (BNT = (*R*)-1, 1′-binaphthalene-2,2′-dithiol)], which could produce H_2 with 676 TONs in CH_3CN/H_2O (1 : 1, v/v) after 4 h of irradiation.[13h] Chen and co-authors reported a Ni complex, $Ni_2(MBD)_4$ (MBD = 2-mercaptobenzimidazole), showing 101 TONs in CH_3CN/H_2O (1 : 1, v/v) after 5 h of irradiation.[13c] The ligands seem to help efficent electron transfer.

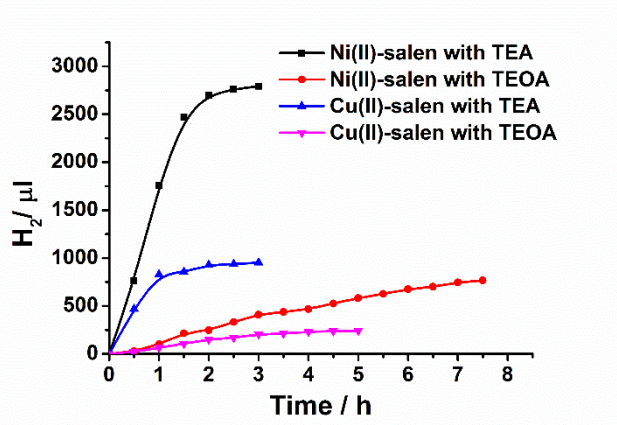

Figure 2. Time dependence of photocatalytic H_2 evolution from the systems containing Ni(II)-salen or Cu(II)-salen complexes (0.1 mM) and TEA or TEOA (10% v/v) in MeOH/H_2O (1: 2, v/v) solution with EY^{2-} (1 mM).

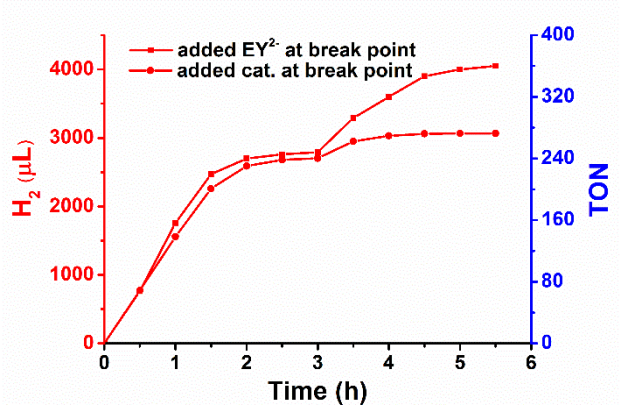

Figure 3. Comparison of the H_2 production against irradiation time by adding extra EY^{2-} (1 mM) and Ni(II)-salen (0.1 mM). The beginning system contains Ni(II)-salen (0.1 mM), EY^{2-} (1 mM) and 10% TEA, at pH 10.

Changing the electron donor from TEA to TEOA, while keeping the Ni(II)-salen and EY^{2-} invariant, notably decreases the activity of the system (Figure 2), as indicated by consistently lower H_2 amounts. However, the duration time can be increased from less than 3 h to more than 8 h. A similar situation also presents in Cu(II)-salen system. The break for H_2 evolution is probably due to

the decomposition of EY^{2-} and metal-salen complexes.[14b] Further study with a system composed of Ni(II)-salen, EY^{2-} and TEA showed that the recovery of hydrogen production was possible by adding extra EY^{2-} (achieve a TON of 362 after another 2.5 h), yet cannot reach the activity as the beginning system (Figure 3), which means there were other factors responsible for the deactivation of hydrogen production, probably was the decomposition of Ni(II)-salen. Supplement of Ni(II)-salen at the breaking point could reproduce hydrogen but with much less efficiency. The recovery investigation indicates that EY^{2-} decomposed much faster than the catalyst in the photolysis progress, and the decomposition of both was responsible for the deactivation of hydrogen production.

Issues related to the stability of the photocatalytic system

During the photocatalytic H_2 evolution processes, it was noticed that the H_2 evolution stopped in the EY^{2-}/Ni(II)-salen/TEA system after 3 h irradiation (Figure 2). However, the H_2 evolution kept going on in the EY^{2-}/Ni(II)-salen/TEOA after 7 h. The deactivation which may be attributed to photochemical damage of the catalyst and the photosensitizer. During the photolysis process, the color immediately changed from orange to yellow green in systems utilizing EY^{2-} as chromophores once starting irradiation and faded even to colorless after 3 h, which is similar to the reported phenomena.[17e] Time-resolved UV-vis spectra were used to investigate the deactivation processes. In a system containing EY^{2-} ($1x10^{-3}$ M), Ni(II)-salen ($1x10^{-4}$ M) and TEA or TEOA (10%, v/v) at pH 10 under 420 nm LED illumination, the UV-vis spectra were recorded after being diluted 30 times (Figure 4). It can be seen that the strong absorption peak of EY^{2-}at 520 nm shifted to 494 nm after being irradiated for 5 mins in both the systems containing TEA and TEOA, which corresponds to their color change from orange to yellow green (Figure S2). Then the absorption decreased as time goes on, however, the system containing TEA presented faster decline than that containing TEOA, more than 95% of the absorption had decreased after 2 h in the TEA system while the absorption decreased less than 60% in the TEOA system. The faster decomposition of chromophore should be responsible for the relatively quick deactivation of H_2 evolution in the system containing TEA compared to the system containing TEOA.

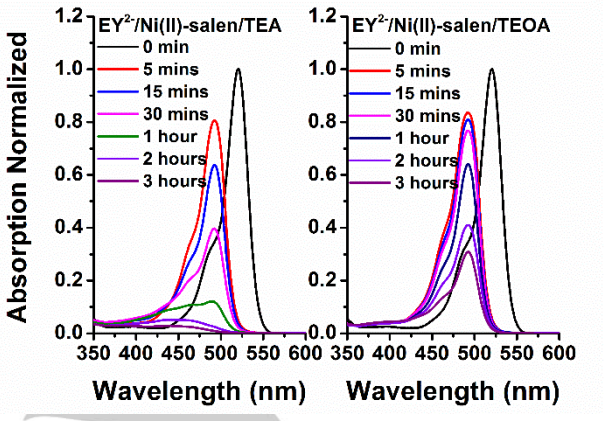

Figure 4. Changes in the absorption spectra under irradiation for the photolysis system containing EY^{2-} (10^{-3} M), Ni(II)-salen (10^{-4} M) and 10% TEA or TEOA after being diluted 300 times. The spectra were normalized by the absorption of EY^{2-} at 520 nm.

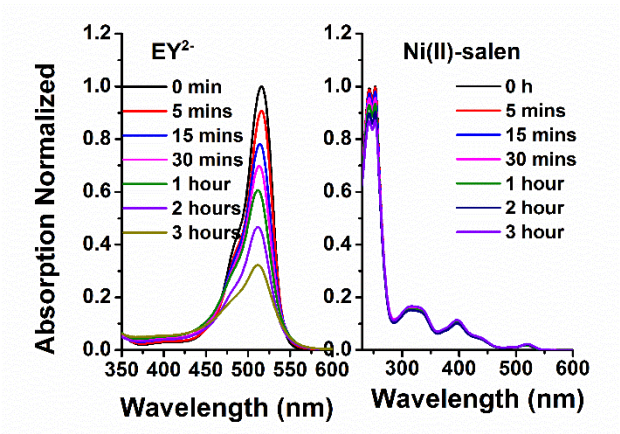

Figure 5. Changes in the absorption spectra under irradiation for the system containing only EY^{2-} (10^{-3} M) or Ni(II)-salen (10^{-4} M) after being diluted 300 times. The spectra were normalized by the absorption of EY^{2-} at 520 nm.

Further investigation of photodecomposition of EY^{2-} and Ni(II)-salen separately, we found that Ni(II)-salen is much more stable than EY^{2-}, only 12% decomposition for Ni(II)-salen was found under irradiation for 3 h while nearly 70% decomposition for EY^{2-} was found (Figure 5). However, single EY^{2-} presented relatively more stable than EY^{2-} in photocatalytic hydrogen evolution systems, indicating that the addition of Ni(II)-salen or TEA could speed up the decomposition of EY^{2-}. Indeed, the addition of Ni(II)-salen into EY^{2-} made the absorption of EY^{2-} decrease dramatically under irradiation (Figure 6), near 95% decline was found after 1 h while only 40% decline was found in the single EY^{2-} system. The absorption of EY^{2-} decrease much more dramatically under irradiation when TEA was added into EY^{2-}. Meanwhile the absorption peak at 520 nm shifted to 494 nm, which is constant with the whole hydrogen evolution system but not found in only EY^{2-} system or EY^{2-} + Ni(II)-salen system (Figure 6). The photos of corresponding solutions are presented in Figure S2-S6. This should be attributed to the cleavage of C-Br through reductive quenching, leading to photodecomposition of EY^{2-} and deterioration of hydrogen evolving activity.[24] While adding Ni(II)-salen into an EY^{2-} + TEA system could greatly prolong the durability of the PS (Figure 4), which was attributed to the electron transfer from PS^{-} to the catalyst and subsequent proton reduction to H_2.[14a, 15, 25] Previously, we found the absorption peak of EY^{2-} shifted to the same position with that of Fl^{2-}, probably following the dehalogenation process under irradiation.[17e] HPLC results from Shimidzuln's work showed that the dehalogenated EY^{2-} presented the same retention time with that of Fl^{2-}.[24a] Here, we investigated dehalogenation in control systems. By means of gravimetry with silver nitrate after 2 h photolysis, the Br^{-} from EY^{2-} were detected (Table 1). As a result, the detected halide ions yield could not reach the degradation extent of EY^{2-}. For example, in single EY^{2-} system, when 54% decomposition of EY^{2-} was observed by UV-vis measurement, only 23% Br^{-} ions were detected by gravimetry. The same situation was also found in other control systems. This means a non-complete cleavage of Br

from EY^{2-} as its decomposition. Moreover, obviously more Br^- ions were detected in systems containing TEA than that without TEA, which means TEA trends to make EY^{2-} lose Br atoms more easily. The UV-vis absorption shift and fast color change in photolysis systems containing TEA enhance this viewpoint. Further, in a complete hydrogen evolution system containing EY^{2-}, Ni(II)-salen and TEA, the Br^- was detected by gravimetry of AgBr in course of time (Figure 7). Obvious Br^- ions were detected at the beginning of irradiation, and most of the Br^- was detected in the first hour and over 80% Br^- ions were detected in 3 h.

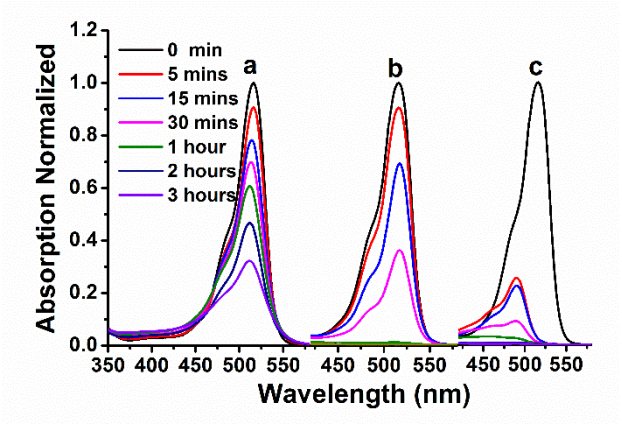

Figure 6. Changes in the absorption spectra under irradiation for the system containing a) only EY^{2-} (10^{-3} M), b) EY^{2-} (10^{-3} M) + Ni(II)-salen (10^{-4} M), c) EY^{2-} (10^{-3} M) + TEA (10% v/v, right) after being diluted 300 times. The spectra were normalized by the absorption of EY^{2-} at 520 nm.

Table 1. Precipitate produced in systems after irradiating for 2 h by adding enough silver nitrate without tuning pH.

Systems	EY^{2-}	EY^{2-} + Ni(II)-salen	EY^{2-} + TEA	EY^{2-} + TEA+ Ni(II)-salen
Precipitate	0.5 mg	1.01 mg	1.71 mg	1.78 mg
Yield	23%	46%	78%	81%
UV-vis Abs. decrease	54%	98%	95%	95%

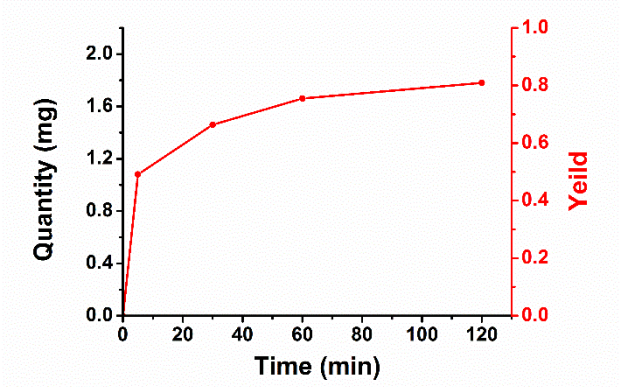

Figure 7. Precipitate produced in 3 mL systems containing only EY^{2-} (10^{-3} M), Ni(II)-salen (10^{-4} M), TEA (10% v/v) by adding enough silver nitrate without tuning pH in course of irradiation time.

Photo-induced electron transfer study

Steady-state fluorescence titration experiments revealed quenching of the fluorescence of EY^{2-} by Ni(II)-salen in water/MeOH (2/1, v/v). On excitation at 400 nm, the EY^{2-} showed an emission peak centered at 540 nm in MeOH/H_2O (1/2, v/v) mixed solution at pH 10, corresponding to $S_1 \rightarrow S_0$ transitions. The difference in energy of the absorption and emission peaks shows a small Stokes shift of 25 nm (Figure S7). The emission peak of EY^{2-} could be quenched dramatically by ca. 50% upon addition of 70 equiv of Ni(II)-salen (Figure S8). This means a favorable oxidative quenching of EY^{2-} by Ni(II)-salen (presumably oxidative quenching to form EY^- + [Ni catalyst]$^-$). To gain further insight into the mechanism of quenching, we performed a Stern–Volmer analysis of the obtained fluorescence titration data. By plotting I_0/I (ratio of fluorescence intensity in the absence or the presence of Ni(II)-salen) against the concentration of Ni(II)-salen (quencher), a linear Stern-Volmer plot was got, indicating a dynamic quenching takes place (Figure S8).[26] A rate constant k_q = 8.27 x 10^6 $M^{-1}s^{-1}$ was calculated. In the previous studies, it was found that the fluorescence of ^{1}*EY^{2-} could not be reductively quenched by the electron donor TEA, while the ^{3}*EY^{2-} could be reductively quenched by TEA, resulting in the formation of the EY^{3-} and TEA^+.[13b] We demonstrated the reductive quenching of EY^{2-} by TEA (Figure S9), which presented a slight quenching in the presence of 700 equiv and a rate constant of 6.04 x 10^4 $M^{-1}s^{-1}$ (Figure S9, 10^2 times lower than that quenched by Ni(II)-salen). However, in the present hydrogen production systems, the concentration of TEA is 0.14 M, more than 10^4 times higher than the concentration of Ni(II)-salen (1 x 10^{-5} M). Therefore, the reductive quenching process dominated the quenching process. The UV-vis spectra investigation for the H_2 evolution system and its obvious color change revealed that the electron transfer from TEA to ^{3}*EY^{2-} happened as soon as irradiation, accompanied with the dehalogenation reaction. The reductive quenching pathway involves PS* and the electron donor and the subsequent electron transfer from PS^- to the catalyst.

Electrocatalytic hydrogen production based on Ni(II)-salen

To elucidate the redox behavior of the catalyst, Ni(II)-salen was subjected to electrochemical investigations in dimethylformamide (DMF). Figure 8a shows the cyclic voltammogram of Ni(II)-salen (1 mM in 0.1 M $TBAPF_6$ in DMF) at a glassy carbon electrode. There is a quasi-reversible couple at 0.10 V (ΔE_p = 72 mV), which are assigned to Ni(II)/Ni(I) couple. A plot of the redox peaks current against the scan rate yielded a straight line, indicative of a diffusion-controlled process (Figure 8b and 8c). Upon addition of trifluoroacetic acid (TFA, pK_a = 6.0 ± 0.3 in DMF),[27] a catalytic wave rose at the reduction potential of the Ni(II)/Ni(I) couple (-1.62 V *vs.* Ag/AgCl) suggests that Ni(I)-salen reduced protons to H_2 (Figure 8e). Besides, a new catalytic wave appears at more positive potential, which should be a ligand-participated reactivity, rendering the ligand noninnercent.[28] It has been proved that, for metal-salen complexes in acidic condition, the M-O could be broken and protonated to form O-H.[29] The coordinated O atoms probably also play a role of proton relay in the catalytic process, which is similar to the situation that the N atom in nickel(II) thiolate complexes plays a role of proton relay.reported by Richard Eisenberg.[14b] When 1 equiv TFA was added in the Ni(II)-salen solution, no catalytic wave was found near Ni(II)/Ni(I) couple, while a new irreversible reductive wave near -0.65 V appeared

(Figure 8d). We tentatively assign this peak to a "Ni(II)HL"/"Ni(I)HL" (L is salen ligand) couple formed in situ through protonation of the original complexes. This might be reasonably attributed to a proton-coupled electron transfer by the protonation of the salen ligand. Thus the mechanism was supposed to be a ligand-assisted metal-centered reactivity for proton reduction,[28] in which Ni(I)HL is an active species. With further addition of TFA, a catalytic wave is seen at a more negative potential (with an onset potential -0.71 V *vs.* Ag/AgCl) than the "Ni(II)HL"/"Ni(I)HL" couple. This observation is consistent with the proposed mechanism involving the further reduction of the initial "Ni(I)HL" intermediate for hydrogen production.[14b] The catalytic peak current follows a linear correlation with respect to [TFA] (Figure 8f), indicating the reaction rate has a second-order dependence on [H^+].[30] This implies that the second protonation step occurs at or before the turnover limiting step (Scheme 2, step 3).[14b] The second reduction (e.g. -1.37 V), at which the catalytic current is seen, leads to formation of a proposed Ni hydride intermediate. Thus, a CECE mechanism is proposed. The overall catalytic rate constant k is estimated to be 7.62 x 10^6 M^{-2} s^{-1}. At a fixed concentration of acid (0.01 M), the peak current varies linearly with the concentration of Ni(II)-salen, indicating a first order dependence on the catalyst concentration (Figure S11). A theoretical half-wave potential value for the reduction of TFA (10 mmol L^{-1}) in DMF is -0.46 V *vs.* Ag/AgCl.[27] Considering the onset potential of -0.71 V *vs.* Ag/AgCl for the catalytic wave under similar conditions, thus an overpotential requirement for H_2 evolution catalyzed by Ni(II)-salen should be at least 250 mV. Controlled potential electrolysis of Ni(II)-salen in 0.1 M TFA in DMF at -1.6 V *vs* Ag/AgCl followed by analysis of the gas in the headspace by GC/TCD showed that H_2 was produced, with >95% Faradaic yield, a TON of 3160 and a TOF of 1580 h^{-1} (Figure S12).

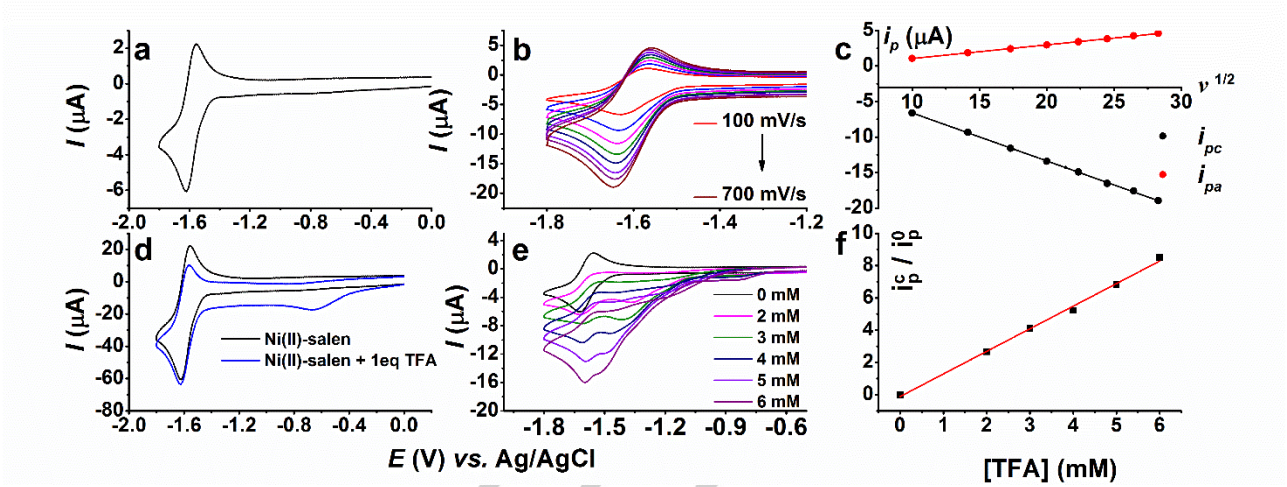

Figure 8. a) CV characterization of Ni(II)-salen (1 mM) in DMF; b) CVs at various scan speeds showing the redox waves; c) plot of the peak current of the first redox wave against the scan speed; d) CV of 1 mM of Ni(II)-salen in DMF without acid and with 1eq TFA; e) CV of 1 mM of Ni(II)-salen in DMF without acid (black) and with TFA titration; f) plot of i_c taken from the peak versus [TFA]. All the systems use $TBAPF_6$ (0.1 M) as the electrolyte, all the potentials are versus Ag/AgCl.

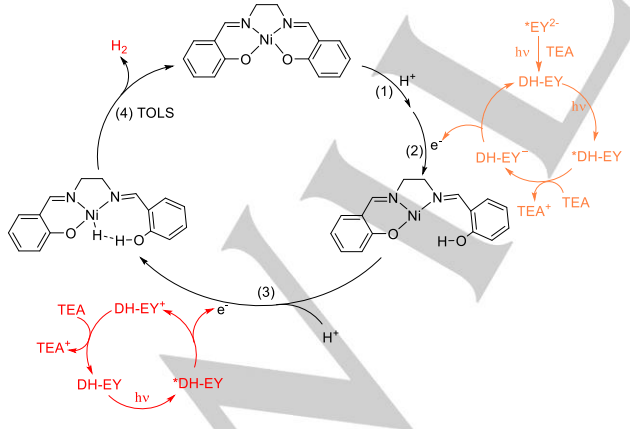

Scheme 2. Proposed mechanism of hydrogen formation. The reversibility of the steps in the scheme beyond the initial protonation has not been established. TOLS = turnover-limiting step.

Mechanism of photocatalytic proton reduction

The above results show that Ni(II)-salen has a reductive potential for $Ni^{II/I}$ at -1.62 V vs. Ag/AgCl. We also studied the redox potential of EY^{2-} with CV measurements (Figure S13), and the first reductive potential E_{red} = −0.75 V and the fist oxidative potential E_{ox} = 0.87 V were found, which is approximate to the FI^{2-} (the complete dehalogenated species). So, it is not possible to receive an electron from EY^{3-} due to the thermodynamical forbiddance. Considering the E_{00} energy of 2.35 eV and 2.30 eV corresponding to the singlet excited state (^{1}*EY^{2-}) and triplet excited state (^{3}*EY^{2-}) of EY^{2-} respectively, the oxidative potential of the two excited states of ^{1}*E_{ox}= −1.48 V and ^{3}*E_{ox} = −1.43 V were obtained (Table S1), which also means a thermodynamically forbidden oxidative quenching process by Ni(II)-salen. However, in the electrochemistry study, a ligand-participated reactivity for H_2 production was found, in which Ni(II)-salen firstly suffered from protonation and then started catalytic performance at -0.71 V. According to this potential, it is possible for Ni(II)-salen to receive a proton from solution and an electron from the EY^{3-} to form Ni(I)HL, while, for the second protonation and reduction to form Ni hydride (with a reductive potential more negative than -1.37 V),

an oxidative quenching should be reasonable. As we illustrated above, the reductive quenching process by TEA to form EY^{3-} is dominating, and the following electrotransfer to a Ni(II)HL is thermodynamically favorable. Therefore, we speculated an initial reductive quenching of $^{3*}EY^{2-}$ by TEA, generating EY^{3-} which then suffered from dehalogenation (DH) process immediately. However, the halogen atoms could not be completely cleaved immediately as the irradiation starting on. The detection for Br^- by gravity method has shown that the cleavage of Br from EY^{2-} is a dramatic but continuous process. So, we name the dehalogenated EY^{2-} in ambiguous extents as DH-EY to represent real and effective PS species. The excited *DH-EY could 1) receive an electron from TEA to form $DH\text{-}EY^{-}$ or 2) transfer electrons to Ni(I)HL to form $DH\text{-}EY^{+}$, followed by the catalytic H_2 production (Scheme 2). Ni(II)-salen firstly suffered from protonation and reduction to form a Ni(I)HL species, then suffered from the second protonation and reduction to form Ni hydried intermediate which will release a H_2 and return to Ni(II)-salen.

Conclusions

Three metal-salen (Ni, Cu and Zn) complexes as catalysts were firstly introduced into homogeneous photocatalytic hydrogen evolution systems. To construct noble-metal-free systems, EY^{2-} was used as photosensitizers instead of the traditional ones containing noble metals. The Ni(II)-salen complex presented much better hydrogen production performance than the other two complexes, with a TON of 362 with one time complement for EY^{2-} in 5.5 h. The stability of the photolysis system was investigated in detail by UV-vis measurements and gravity method. The decomposition of dyes and catalysts should be responsible for the deactivation, and the former was more serious as proved by UV-vis spctra study. The fluorescence quenching experiments showed that the reductive quenching of $^{3*}EY^{2-}$ by receiving an electron from TEA dominated the process, although the reductive quenching by Ni(II)-salen is thermodynamically favorable. Investigation of electrocatalytic proton reduction by Ni(II)-salen showed a CECE mechanism. An overall catalytic rate constant of $7.62 \times 10^6\ M^{-2}\ s^{-1}$ was achieved. Through bulk electrolysis, a Faradaic yield >95% was achieved, with a TON of 3160 and a TOF of 1580 h^{-1}. Based on all the results, a photocatalytic hydrogen evolving mechanism is proposed.

Experimental Section

Materials

According to a method reported in the literature,[31] the salen ligands were synthesized simply and in one step from the reaction of an aldehyde with a diamine. Followed by the reaction with Ni(II), Cu(II), Zn(II) acetate in ethanol, we can get the corresponding complexes. Disodium salts of Eosin Y and tetrabutylammonium hexafluorophosphate ($TBAPF_6$) were purchased from TCI and used without further purification. DMF used for electrochemistry is fresh distilled. Other solvents were of analytical purity and used without further treatment unless otherwise stated.

Photocatalytic activity of hydrogen production

Samples in $MeOH/H_2O$ (1/2; 5.0 mL) containing 0.1 mM catalyst, 1.0 mM EY^{2-}, and TEA (10% v/v) were prepared in 10 mL scintillation vials and protected from light before use. The pH value of the solution was adjusted by adding HCl or NaOH and measured on a FE20-K pH meter. The reaction mixture was degassed by bubbling with high purity N_2 for 15 min to remove air. The photolysis experiments were carried out upon irradiation with a 450 nm LED light (1 W). The gas phase generated from the reaction system was analyzed on a GC SP6890 instrument with a 5 Å molecular sieve column and a thermal conductivity detector using N_2 as the carrying gas, by injecting 100 μL of headspace into the gas chromatograph, and were quantified by a calibration plot to the internal CH_4 standard.

Spectroscopic Measurements

UV−vis spectra in acetonitrile were taken on a Cary 60 UV-vis spectrophotometer using a 1 cm path length quartz cuvette.

Fluorescence Quenching

A solution (2.0 mL) of EY^{2-} at 1 μM concentration in a 1/2 $MeOH/H_2O$ mixture (pH adjusted to 10) was prepared in a quartz cuvette fitted with a septum cap, and the solution was degassed under N_2 for 5 min. Aliquots of 10−100 μL of N_2-degassed solution containing quencher in the same solvent mixture (pH adjusted to 10) were added, and the intensity of the fluorescence was monitored by steady-state fluorescence, exciting at 450 nm on a FP-8500 fluorimeter with a photomultiplier tube detector.

Cyclic Voltammetry

Cyclic voltammetry (CV) measurements of the catalyst were performed with a one-compartment cell with a 1.6 mm diameter glassy-carbon working electrode, a Pt auxiliary electrode, and an Ag/AgCl reference electrode on the BioLogic VSP-300. The electrolyte for electrochemistry in DMF was 0.1 M $TBAPF_6$. Argon was used to purge all samples. In the acid concentration dependence study, a 1.0 M TFA stock solution was prepared in the same solvent mixture with 0.1 M corresponding electrolyte. To a stirred 1.0 mM catalyst solution, the acid stock solution was added, and the mixture was purged with argon for another 5 min before performing cyclic voltammetry.

Catalytic rate constants determination

The peak current (i_p) for the diffusion-controlled electron-transfer process is given by Eq. (1):

$$i_p = nFA[cat]\sqrt{D}\sqrt{(Fv)/RT} \qquad (1)$$

From the slope of the plot of i_p against $v^{1/2}$, the diffusion coefficient (D) can be obtained. The catalytic current for a reversible electron-transfer process followed by a fast catalytic reaction (E_RC_{cat}) is given by Eq. (2):

$$i_c = nFA[cat]\sqrt{Dk[H]^2} \qquad (2)$$

At low-acid concentration the plot of i_c against acid concentration is linear and the overall catalytic rate constant can be obtained from the slope of the plot.

The feasibility analysis of photo-induced electron transfer processes

Firstly, the first redox potential of EY^{2-} (E_{red} and E_{ox}) was confirmed by CV measurement. Secondly, the exciting energy of EY^{2-} ($E_{0,0}$) was calculated from the crossing wavelength of its UV-vis absorption and Fluorescence. The oxidative potential of excited state: $^*E_{ox} = E_{ox} - E_{0,0}$; the reductive potential of excited state: $^*E_{red} = E_{red} + E_{0,0}$;

Then, the Gibbs free energy (ΔG^0) of oxidative process was calculated by this equation: $\Delta G^0 = {}^*E_{ox} - E_{red}(Q)$; the Gibbs free energy (ΔG^0) of the reductive process was calculated by this equation: $\Delta G^0 = E_{ox}(Q) - {}^*E_{red}$

Acknowledgements

We are grateful to the funding support from Shaanxi Provincial Education Department (No 15JK1708), Shannxi Provincial Science & Technology Department (No 2017JQ2012), China Scholarship Council and Top-rated Discipline construction scheme of Shaanxi higher education.

Keywords: photocatalysis • electrocatalysis • hydrogen • metal-salen complex • nickel

[1] a) Y. Wang, A. Vogel, M. Sachs, R. Sprick, L. Wilbraham, S. Moniz, R. Godin, M. Zwijnenburg, J. Durrant, A. Cooper, J. Tang, *Nature Energy*, **2019**, 4, 746-760; b)D. Kong, Y. Zheng, M. Kobielusz, Y. Wang, Z. Bai, W. Macyk, X. Wang, J. Tang, *Mater. Today* **2018,** 21 (8), 897-924.

[2] a) M. S. Faber, S. Jin, *Energy Environ. Sci.* **2014**, *7*, 3519-3542; b) J. Wang, W. Cui, Q. Liu, Z. Xing, A. M. Asiri, X. Sun, *Adv. Mater.* **2015**.

[3] a) S. Berardi, S. Drouet, L. Francas, C. Gimbert-Surinach, M. Guttentag, C. Richmond, T. Stoll, A. Llobet, *Chem. Soc. Rev.* **2014**, *43*, 7501-7519; b) J. Willkomm, K. L. Orchard, A. Reynal, E. Pastor, J. R. Durrant, E. Reisner, *Chem. Soc. Rev.* **2016**, *45*, 9-23; c) C. Jiang, S. Moniz, A. Wang, T. Zhang, J. Tang, *Chem. Soc. Rev.* **2017**, 46 (15), 4645-4660; d) C. Jiang, S. Moniz, M. Khraisheh, J. Tang, *Chem. Eur. J.* **2014**, 20 (40), 12954-12961.

[4] a) Z.-J. Li, X.-B. Li, J.-J. Wang, S. Yu, C.-B. Li, C.-H. Tung, L.-Z. Wu, *Energy Environ. Sci.* **2013**, *6*, 465-469; b) Z. Yang, M. Pang, S.-G. Xia, X.-Y. Gao, Q. Guo, X.-B. Li, C.-H. Tung, L.-Z. Wu, W. Wang, *ChemPhotoChem* **2019**, *3*, 220-224.

[5] M. L. Helm, M. P. Stewart, R. M. Bullock, M. R. DuBois, D. L. DuBois, *Science* **2011**, *333*, 863-866.

[6] W. Lubitz, H. Ogata, O. Rüdiger, E. Reijerse, *Chem. Rev.* **2014**, *114*, 4081-4148.

[7] a) Y.-J. Yuan, Z.-T. Yu, D.-Q. Chen, Z.-G. Zou, *Chem. Soc. Rev.* **2017**; b) F. Möller, S. Piontek, R. G. Miller, U.-P. Apfel, *Chem. Eur. J.* **2018**, *24*, 1471-1493.

[8] a) P. Du, K. Knowles, R. Eisenberg, *J. Am. Chem. Soc.* **2008**, *130*, 12576-12577; b) W.-G. Wang, F. Wang, H.-Y. Wang, C.-H. Tung, L.-Z. Wu, *Dalton Trans.* **2012**, *41*, 2420-2426.

[9] a) K. Kalyanasundaram, *Coord. Chem. Rev.* **1982**, *46*, 159-244; b) S. Ott, M. Kritikos, B. Åkermark, L. Sun, *Angew. Chem. Int. Ed.* **2003**, *42*, 3285-3288; c) H. Wolpher, M. Borgström, L. Hammarström, J. Bergquist, V. Sundström, S. Styring, L. Sun, B. Åkermark, *Inorg. Chem. Commun.* **2003**, *6*, 989-991; d) Y. Na, M. Wang, J. Pan, P. Zhang, B. Åkermark, L. Sun, *Inorg. Chem.* **2008**, *47*, 2805-2810; e) W. Gao, J. Sun, T. Åkermark, M. Li, L. Eriksson, L. Sun, B. Åkermark, *Chem. Eur. J.* **2010**, *16*, 2537-2546; f) Y. Sano, A. Onoda, T. Hayashi, *Chem. Commun.* **2011**, *47*, 8229-8231; g) W.-N. Cao, F. Wang, H.-Y. Wang, B. Chen, K. Feng, C.-H. Tung, L.-Z. Wu, *Chem. Commun.* **2012**, *48*, 8081-8083.

[10] a) F. Gärtner, B. Sundararaju, A.-E. Surkus, A. Boddien, B. Loges, H. Junge, P. H. Dixneuf, M. Beller, *Angew. Chem. Int. Ed.* **2009**, *48*, 9962-9965; b) H.-h. Cui, M.-q. Hu, H.-m. Wen, G.-l. Chai, C.-b. Ma, H. Chen, C.-n. Chen, *Dalton Trans.* **2012**, *41*, 13899-13907; c) C.-F. Leung, S.-M. Ng, C.-C. Ko, W.-L. Man, J. Wu, L. Chen, T.-C. Lau, *Energy Environ. Sci.* **2012**, *5*, 7903-7907; d) T. Yu, Y. Zeng, J. Chen, Y.-Y. Li, G. Yang, Y. Li, *Angew. Chem. Int. Ed.* **2013**, *52*, 1-6.

[11] F. Wang, W.-J. Liang, W.-G. Wang, B. Chen, K. Feng, L.-P. Zhang, C.-H. Tung, L.-Z. Wu, *Acta Chim. Sinica* **2012**, *70*, 2306-2310.

[12] a) W. Gao, J. Liu, W. Jiang, M. Wang, L. Weng, B. Åkermark, L. Sun, *C.R. Chim.* **2008**, *11*, 915-921; b) H.-Y. Wang, W.-G. Wang, G. Si, F. Wang, C.-H. Tung, L.-Z. Wu, *Langmuir* **2010**, *26*, 9766-9771; c) M. Guttentag, A. Rodenberg, R. Kopelent, B. Probst, C. Buchwalder, M. Brandstätter, P. Hamm, R. Alberto, *Eur. J. Inorg. Chem.* **2012**, *2012*, 59-64; d) J.-H. Liu, W.-N. Jiang, *Dalton Trans.* **2012**, *41*, 9700-9707; e) A. Rodenberg, M. Orazietti, B. Probst, C. Bachmann, R. Alberto, K. K. Baldridge, P. Hamm, *Inorg. Chem.* **2014**, *54*, 646-657; f) W.-G. Wang, F. Wang, H.-Y. Wang, G. Si, C.-H. Tung, L.-Z. Wu, *Chem. Asian J.* **2010**, *5*, 1796-1803.

[13] a) J. Dong, M. Wang, P. Zhang, S. Yang, J. Liu, X. Li, L. Sun, *J. Phys. Chem. C* **2011**, *115*, 15089-15096; b) X. Li, M. Wang, D. Zheng, K. Han, J. Dong, L. Sun, *Energy Environ. Sci.* **2012**, *5*, 8220-8224; c) H.-h. Cui, J.-y. Wang, M.-q. Hu, C.-b. Ma, H.-m. Wen, X.-w. Song, C.-n. Chen, *Dalton Trans.* **2013**, *42*, 8684-8691; d) C. Orain, F. Quentel, F. Gloaguen, *ChemSusChem* **2014**, *7*, 638-643; e) H. Rao, Z.-Y. Wang, J. Wang, X.-Z. Hu, Y.-T. Fan, H.-W. Hou, *Int. J. Energy Res.* **2014**, *38*, 2003-2009; f) X.-Z. Hu, H.-Q. Zheng, H. Rao, C.-M. Pan, Y.-T. Fan, *J. Energy Inst.* **2015**, *88*, 359-363; g) H. Rao, Z.-Y. Wang, H.-Q. Zheng, X.-B. Wang, C.-M. Pan, Y.-T. Fan, H.-W. Hou, *Catalysis Science & Technology* **2015**, *5*, 2332-2339.

[14] a) Z. Han, W. R. McNamara, M.-S. Eum, P. L. Holland, R. Eisenberg, *Angew. Chem. Int. Ed.* **2012**, *51*, 1667-1670; b) Z. Han, L. Shen, W. W. Brennessel, P. L. Holland, R. Eisenberg, *J. Am. Chem. Soc.* **2013**, *135*, 14659-14669.

[15] T. M. McCormick, B. D. Calitree, A. Orchard, N. D. Kraut, F. V. Bright, M. R. Detty, R. Eisenberg, *J. Am. Chem. Soc.* **2010**, *132*, 15480-15483.

[16] J. Han, W. Zhang, T. Zhou, X. Wang, R. Xu, *RSC Adv.* **2012**, *2*, 8293-8296.

[17] a) P. Zhang, M. Wang, J. Dong, X. Li, F. Wang, L. Wu, L. Sun, *J. Phys. Chem. C* **2010**, *114*, 15868-15874; b) S. Gao, S. Huang, Q. Duan, J. Hou, D. Jiang, Q. Liang, J. Zhao, *Int. J. Hydrogen Energy* **2014**, *39*, 10434-10444; c) R. P. Sabatini, B. Lindley, T. M. McCormick, T. Lazarides, W. W. Brennessel, D. W. McCamant, R. Eisenberg, *J. Phys. Chem. B* **2016**, *120*, 527-534; d) S. Gao, W.-Y. Zhang, Q. Duan, Q.-C. Liang, D.-Y. Jiang, J.-X. Zhao, J.-H. Hou, *Chem. Pap.* **2017**, *71*, 617-625; e) C.-B. Li, P. Gong, Y. Yang, H.-Y. Wang, *Catal. Lett.* **2018**, *148*, 3158-3164.

[18] a) E. Mejía, S.-P. Luo, M. Karnahl, A. Friedrich, S. Tschierlei, A.-E. Surkus, H. Junge, S. Gladiali, S. Lochbrunner, M. Beller, *Chem. Eur. J.* **2013**, *19*, 15972-15978; b) M. Natali, R. Argazzi, C. Chiorboli, E. Iengo, F. Scandola, *Chem. Eur. J.* **2013**, *19*, 9261-9271.

[19] S. C. Eady, S. L. Peczonczyk, S. Maldonado, N. Lehnert, *Chem. Commun.* **2014**, *50*, 8065-8068.

[20] S. J. Wezenberg, A. W. Kleij, *Angew. Chem. Int. Ed.* **2008**, *47*, 2354-2364.

[21] P. G. Cozzi, *Chem. Soc. Rev.* **2004**, *33*, 410-421.

[22] R. M. Clarke, T. Storr, *Dalton Trans.* **2014**, *43*, 9380-9391.

[23] a) H. Chen, Z. Sun, S. Ye, D. Lu, P. Du, *J. Mater. Chem. A* **2015**, *3*, 15729-15737; b) R. M. Irfan, D. Jiang, Z. Sun, L. Zhang, S. Cui, P. Du, *J. Catal.* **2017**, *353*, 274-285.

[24] a) T. Shimidzu, T. Iyoda, Y. Koide, *J. Am. Chem. Soc.* **1985**, *107*, 35-41; b) C. R. Lambert, I. E. Kochevar, *Photochem. Photobiol.* **1997**, *66*, 15-25; c) W. Zhang, J. Hong, J. Zheng, Z. Huang, J. Zhou, R. Xu, *J. Am. Chem. Soc.* **2011**, *133*, 20680-20683.

[25] W. T. Eckenhoff, R. Eisenberg, *Dalton Trans.* **2012**, *41*, 13004-13021.

[26] H.-x. Zhang, P. Mei, X.-x. Yang, *"Spectrochim. Acta, Part A "* **2009**, *72*, 621-626.

[27] V. Fourmond, S. Canaguier, B. Golly, M. J. Field, M. Fontecave, V. Artero, *Energy Environ. Sci.* **2011**, *4*, 2417-2427.

[28] T. Straistari, J. Fize, S. Shova, M. Réglier, V. Artero, M. Orio, *ChemCatChem* **2017**, *9*, 2262-2268.

[29] J. Cheng, F. Gou, X. Zhang, G. Shen, X. Zhou, H. Xiang, *Inorg. Chem.* **2016**, *55*, 9221-9229.

[30] J.-M. Savéant, *Elements of Molecular and Biomolecular Electrochemistry: An Electrochemical Approach to Electron Transfer Chemistry*, John Wiley & Sons: Hoboken, **2006**, p. 109.

[31] a) B. Rhodes, S. Rowling, P. Tidswell, S. Woodward, S. M. Brown, *J. Mol. Catal. A: Chem.* **1997**, *116*, 375-384; b) M. T. Räisänen, H. Korpi, M. R. Sundberg, A. Savin, M. Leskelä, T. Repo, *Inorg. Chim. Acta* **2013**, *394*, 203-209.

Entry for the Table of Contents (Please choose one layout)

FULL PAPER

Ideal hydrogen production systems would require minimal synthetic effort and use inexpensive compounds. Cheap metal-salen complexes, with merits of easy preparation, readily tunable ligands and high activity for catalytic hydrogen production, have been proved to be good candidates for large scale H_2 economy while the stability and understanding of the catalytic mechanism for the H_2 evolution should be further improved

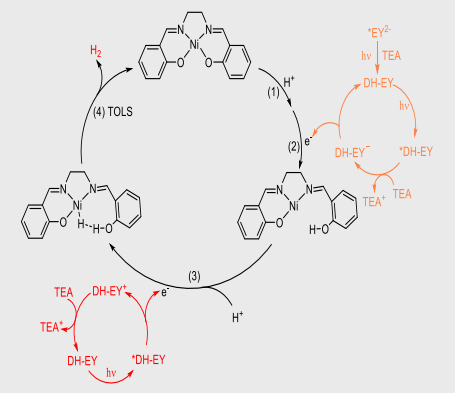

*Author(s), Corresponding Author(s)**

Page No. – Page No.

Title